Proceedings of ERAD (2004): 216–222 © Copernicus GmbH 2004

ERAD 2004

Impact of combined beam blocking and anomalous propagation correction algorithms on radar data quality

A. Fornasiero[1,2], **R. Amorati**[2], **P. P. Alberoni**[2], **L. Ferraris**[1,3], **and A. C. Taramasso**[1,3]

[1]CIMA Università di Genova e della Basilicata, Savona, Italy
[2]A.R.P.A Emilia-Romagna – Servizio Idrometeorologico Regionale, Bologna, Italy
[3]DIST Università di Genova, Genova, Italy

Abstract. Radar precipitation estimate is affected by several kinds of errors and corruptions, therefore, it is difficult to evaluate its reliability in meteorological applications. The general aim of our work is to reduce such contamination and to identify a data quality flag that resumes the impact of these errors in the final rain rate data.

In this specific context we evaluate the amount of data contamination due to signal interaction with the ground that produces clutter and beam blocking (BB). The attention is focused on its relationship with the variability of the propagation conditions.

We consider as base field, a radar field decluttered through a doppler filter and a clear air static map. We apply on this field an algorithm of anomalous propagation detection based on vertical profile analysis, and than we add one based on the signal propagation model included in the BB correction algorithm. The results of the two algorithms are compared to verify the improvement introduced from the BB and propagation model to resolve different kinds of artifices. The addition of BB correction algorithm produces a change in the original scheme, not only in terms of power loss correction, but even in the choice of the optimum elevations map. Finally we evaluate statistically the improvement introduced by adding BB algorithm in the operational line of radar data correction and consequently the impact of the BB on the data quality, related to the propagation conditions.

1 Introduction

The use of radar rain measurement in a operational way such as data assimilation or data mosaicking needs to define a sequence of preliminary operations to remove data artifices. The correction can be performed trough statistical-empirical analysis or physical-based modelling. Due to the strong variability of the factors that determines the problems, a statistical approach cannot be sufficient to obtain the optimum reflectivity value. This is evident in presence of problems related to the signal propagation that is strong depending on atmospheric conditions of the boundary layer. For example, ground clutter and beam blockage are different form of data contamination that affect reflectivity measure in complex orography. Their common cause is the interaction of the radar signal with the ground. A physical based approach to correct this effects cannot negligee the study and modelling of the radar beam trajectory depending on thermodynamic boundary layer conditions. This approach permit a more efficient real time correction of radar field, that takes into account the operating conditions. But, because of it is based on several assumptions and simplifications (such as negligibility of secondary lobes), it must be integrated with the statistical based pre-processing and with a empirical-statistic post-processing.

Correspondence to: A. Fornasiero
(afornasiero@smr.arpa.it)

2 The radar signal propagation.

In the low troposphere electromagnetic waves do not propagate generally in a straight line; its path is a curve depending on the variation of the refractive index n, which is a function of the temperature and water content. Empirical observations demonstrate that the refractive index gradient in standard conditions and in the first 2 Km of the atmosphere is constant and inversely proportional to the earth radius. In this case the effective earth radius (hypothetic radius that the earth must have, if we consider the ray path as a straight line, to keep the relation between ray height and arc length) is:

$$a_e = 4/3a \tag{1}$$

where a is the earth radius and a_e is the effective earth radius. Usually, for dimensional reasons the propagation conditions are described from the refractivity (N $= n \times 10^6$). For microwave and in the low troposphere, this growth can be estimated through the formula of Bean and Dutton (1968):

$$N = (77.6/T)/(P + 4810 P_w/T) \tag{2}$$

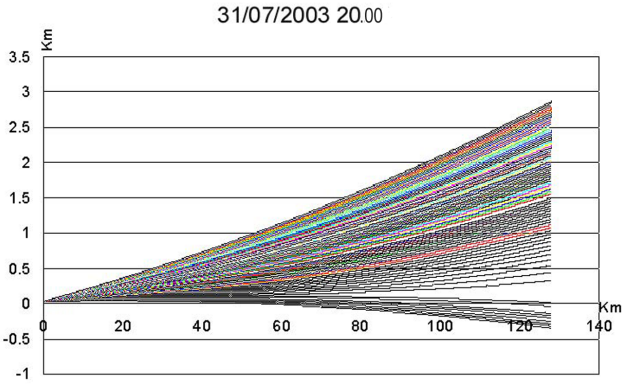

Fig. 1. Beam path at 0.5° antenna elevation. It has been 'broken' the principal lobe in small rays and followed the path of each one.

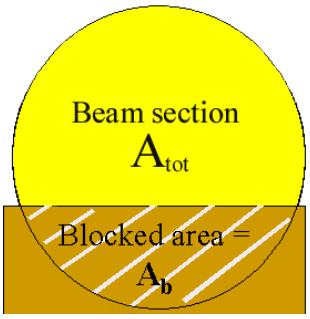

Fig. 2. Beam blockage schema of Bech et al. (2003). The fractional power loss is pBB = A_b/A_{tot}.

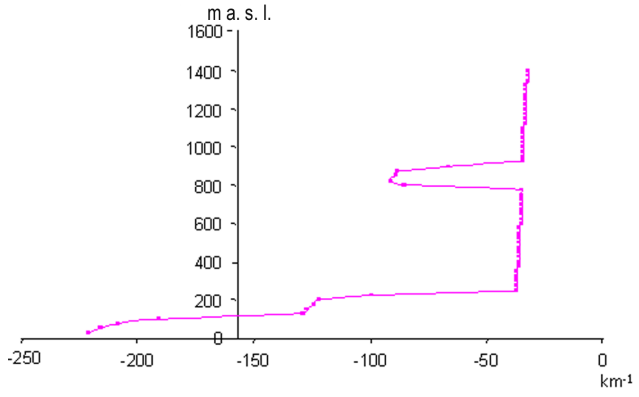

Fig. 3. N gradient profile. Time: 01/08/2003 00.00.

where N is an adimensional number, P is the total pressure, P_w is the partial pressure of water (mbar) and T is the temperature (° Kelvin). In the radar-meteorology applications we consider the firsts kilometres of atmosphere, in this layer the temperature decreases generally with the height and the N gradient is near to the value of -40 km^{-1} (standard conditions). In temperature inversion conditions, this value is often lower than -157 km^{-1} and the ray could bent to the ground. During this phenomenon, called anomalous propagation (hereinafter anaprop), we can, wrongly, attribute clutter echo as meteorological objects and overestimate the rain intensity. Further, the propagation depends strongly on local thermodynamic conditions, which substantially varies in space and time. Anaprop events are generally determined from the thermodynamic conditions of the first 200–300 m of atmosphere. In flat land the radar beam reach this height (relative to the ground) into a distance quite small. As a consequence even if a sounding station is unable to characterize the propagation conditions over the whole radar domain, in flat land, it can be sufficient to recognize anaprop conditions. In our work we have used the TEMP (WMO radiosoundings data format) interpolated at steps of 25 m, to derive the N profile, assuming this description valid in the mountains area too. Once known the N gradient the path of a wave relative to the earth can be calculated through the formula reported in Doviak and Zrnic (1984).

$$h = \sqrt{r^2 + (k_e a)^2 + 2rk_e a \sin\theta} - k_e a + H_0 \qquad (3)$$

where r is the distance from radar, a the Earth's radius, θ the antenna elevation and H_0 the antenna's height; $k_e a$is the effective Earth's radius, which is a function of the N gradient.

3 Clutter and beam blocking removal

3.0.1 The static map

The most simplex and low cost way to avoid clutter echoes in radar rain estimate is the use of maps of clear air (hereinafter CAM), i.e. to keep the Z value from radar scans at different elevations normally (during clear air weather) not affected from ground echoes. This approach is efficient to remove a large rate of contamination affecting data in standard conditions and to avoid the effects of secondary lobes, but never resolve anomalous propagation effects, never takes into account the power loss due to the mountains. Therefore we have integrated this map introducing propagation and beam blockage modelling. Two other maps has been defined, a forecasted clutter elevation map (hereinafter FCEM) and a beam blocking elevation map (hereinafter BBEM) The first is obtained calculating the path of radar beam through the Eq. (2), and overlaying it to a DEM (digital elevation model): scan elevations are chosen in each bin to avoid ground clutter. This map is obtained considering the path of the one-half-power lobe lower limit (and not of the centre) to take into account cases of anomalous propagation. In this cases the beam section does not propagate as a circle, and we cannot derive the points of clutter simply from centre trajectory. It has been observed in the case illustrated in Fig. 1, where we have broken the principal lobe in small rays and followed the ray paths. To describe the form of the beam section it would be necessary a three dimensional model, therefore we have skipped the problem considering directly the path of lower limit.

The second map is chosen in order to grant sufficient power (i.e. at least 50% of transmitted power) reaching each

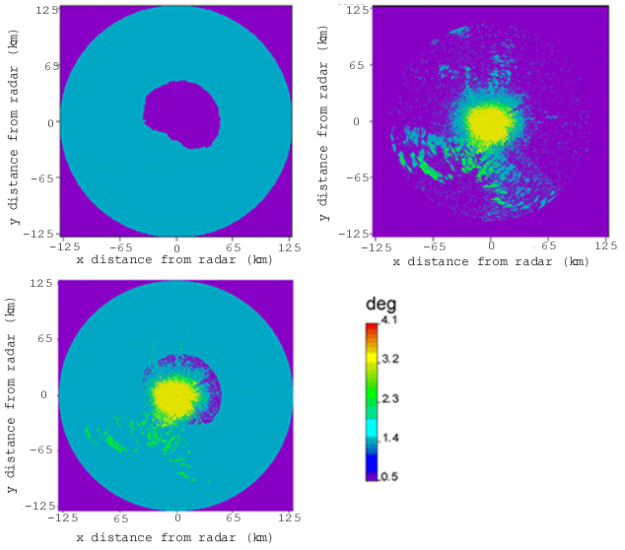

Fig. 4. High panel: BBEM + FCEM (lefts) and static map of clear air CAM (rights). Low panel: final static map. Time: 31/07/2003 20.00.

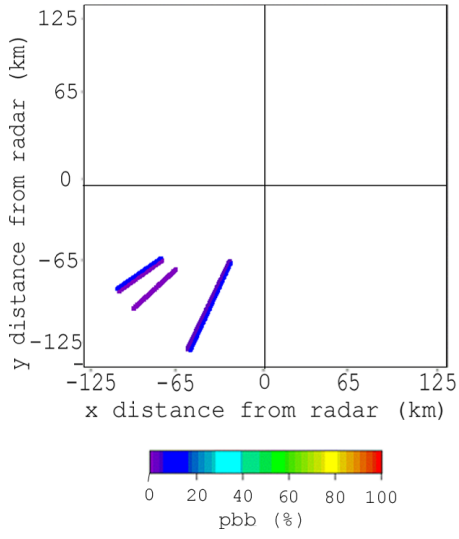

Fig. 5. Percentage of beam blocking. Time: 31/07/2003 20.00.

bin. The beam blocking model based on a geometric-optic approach (Bech et al., 2003) is described in Sect. 3.3 and needs only to know the DTM and the gradient of refractivity. To describe the atmospheric condition we have used the radiosoundings falling in the twelve hours before and after the case. The N profile is calculated as time linear combination of them obtained from the radiosoundings. If the radiosounding is absent, it has been used a standard profile. The final static map contains in each bin the maximum elevation of the three maps.

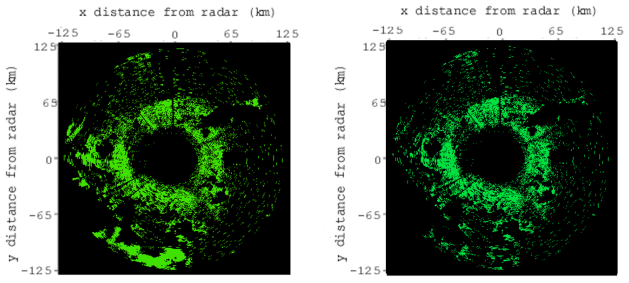

Fig. 6. Anomalous propagation (green), detected from original scheme of Alberoni (left panel) and from new scheme (right panel). Time: 31/07/2003 20.00.

Table 1. Anomalous propagation detection thresholds, for the first bin with anaprop in a azimut and for the sequent bins in the same azimut ('behind anaprop').

Threshold (dbZ)	Standard	Behind anaprop
T1	30	15
T2	−10	0

Table 2. Quality parameters.

Quality parameters	value
Distance bin-soil	m
Corrected beam blocking	%
Removed clutter	Yes/no
Anomalous propagation control	Yes/no
No data	Yes/no

3.1 Removal of residual anomalous propagation clutter

Because of the approximations in the path modelling, such as the spatial uniformity of N profile, and its linear time evolution, is necessary a post elaboration to remove residual clutter due at first to anomalous propagation. The method used in this work has been implemented by Alberoni et al. (2001) and is based on the vertical Z profile analysis. Anomalous propagation is discriminated if the difference between Z value at the elevation of static map and at the successive elevation exceeds the thresholds T1 in Table 1 or if this difference is greater than 0 dbZ and the value at the successive elevation is lower than T2. We have introduced a modification to this scheme, to take into account cases of rain with limited vertical development: at second or successive elevations and after 80 km from radar, the test is applied only if the difference between Z value at previous elevation and at current elevation is greater than a threshold of 10 dBZ (i.e. it is probably present clutter).

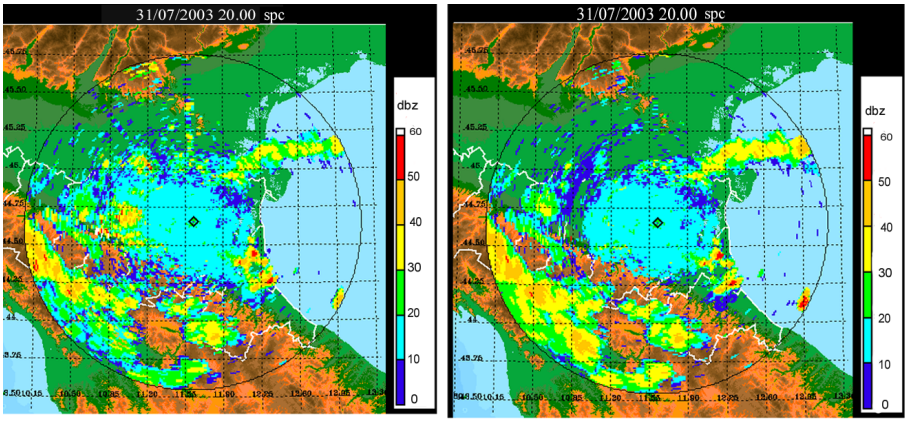

Fig. 7. Left panel: Z map after CAM+VPR analysis correction. Right panel: Z map after the new method correction Time: 31/07/2003 20.00. Increasing reflectivity from blue to red.

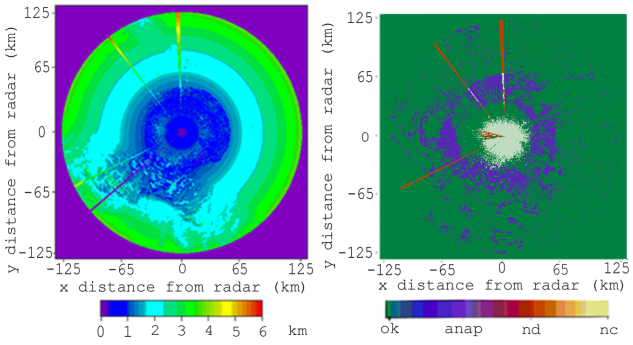

Fig. 8. Left panel: a) bins height relative to the ground. Right panel: b) bins classification; 'anap'=anomalous propagation, 'nd'=no data, 'nc'= no control; Time: 31/07/2003 20.00.

3.2 Beam blocking model

The beam blocking model developed from Bech et al. (2003) is based on a geometric-optic approach, i.e. because of microwaves, such as visible waves are totally absorbed and reflected from ground, is possible to evaluate the power blockage treating them as where light. This model assumes that the main lobe propagates in the atmosphere with a circular section where the power density is uniform. This approximation isn't applicable in anomalous propagation conditions, but it is at the elevations chosen previously in the static map, that are defined to avoid anomalous propagation effects. In fact the exemplum in Fig. 1 shows how, even if the lower part of the beam bent to the soil, the upper part propagate freely in the atmosphere. We can also assume that at the upper elevation the circular section approximation is reliable. The fraction of power lost is so equivalent to the fraction of beam section intercepted from orography as illustrated in Fig. 2

3.3 The combined algorithm and the quality output

The methodology to remove clutter and beam blockage can be resumed in this steps: 1) choice of the combined static map as sum of CAM, FCEM and BBEM 2) correction of the power loss 3) removal of anaprop residual clutter through vertical Z profile analysis of Alberoni et al. modified schema. This order of actions is established for the application of the method in an operative line. For the same scope we have added another step: the production of quality outputs i.e. indicators of the effective reliability of the final reflectivity datum for meteorological applications. It has been defined some parameters assuming quantitative or logical values that are shown in Table 2. The next work will be to find a quality function that takes into account this indicators.

4 Results

The described methodology has been applied and tested on two case studies related to different type of meteorological events. The first is a thunderstorm occurred in summer 2003, on 31 July when anomalous propagation conditions has been verified. The second is a case of stratiform rain occurred in winter 2003, at 10 December in the afternoon. The reflectivity dataset comes from San Pietro Capofiume radar located in Italy, in the Po Valley 30–40 km from the mountains of Appennino. Here is colocated the radiosounding station. We have used the radar scans at min 00, 15, 30, 45, decluttered through Doppler filter and acquired at PRF of 1200 Hz and impulse time of 0.5 μs, i.e. with a range resolution of 75 m, smoothed afterwards at 250 m. The angular width of antenna is 0.9° and its scan elevation are 0.5 ˚ , 1.4°, 2.3°, 3.2°, 4.1°. The performance of the new algorithm has been evaluated, at first qualitatively, comparing it with a method of reflecitivity correction based only on CAM and anaprop removal schema of Alberoni et al. (2001). Thereafter a statistical analysis on the two complete events has been performed to evaluate quantitatively its reliability. To illustrate the operational

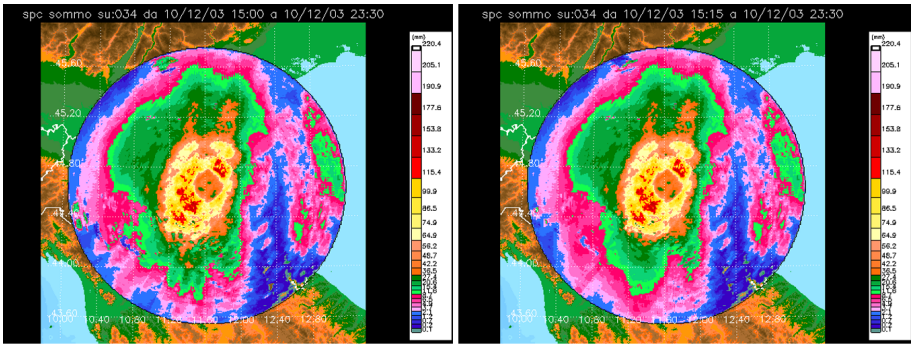

Fig. 9. Map of cumulated rain after CAM+anaprop correction (left panel) and after the new method correction (right panel). Event 10/12/2003 from 15.00 to 23.00. Increasing rain from blue to red.

sequence including the quality output we have chosen an instant of the thunderstorm event with anomalous propagation. In Fig. 3 the N gradient obtained from the nearest radiosounding is represented. A strong temperature inversion causes anaprop in the first 200 m, in fact the value of dN/dh is smaller than $-157\,\mathrm{km}^{-1}$. The form of the radar beam for the elevation of 0.5° is illustrated in Fig. 1 and has been previously discussed. Using this atmospheric description we have defined the FCEM and the BBEM and combining them with the CAM we have obtained the final static map (Fig. 4). In this case, because of the strong anomalous propagation, the elevation is nearly overall greater than the first. At this elevation the modelled beam blockage is almost absent as represented in Fig. 5.

Next step is the removal of anomalous propagation clutter. In Fig. 6 the maps of anaprop obtained from original and modified scheme are represented: at the SO bound of the map a precipitation echo is recognised from the original algorithm as anomalous propagation; the second scheme avoids this error.

Figure 7 shows the reflectivity map at 1km resolution obtained from the method of clutter removal based on CAM and anaprop schema, and that obtained from the new combined method. It appears clear that the new scheme reduces the ground clutter and the blocking effect (beyond the mountains the signal is more continuous). We note in either scheme the presence of secondary lobes echoes. The last step is the production of a set of quality index: the fractional beam blocking (Fig. 4), the map of heights relative to the soil (Fig. 8, lefts) and the bins classification including recognised anomalous propagation (Fig. 8, rights). Once illustrated the operative steps, we have focused the attention on the whole events. The cumulated rain for the stratiform event has been calculated through the two algorithm and represented in Fig. 9. The effect of beam blockage correction is visible, together the remaining problem due to the vertical variation of reflectivity that strongly affect the final result.

Finally we have performed the quantitative-statistical analysis, in the mountain area, since the new algorithm produces its effects mostly in and beyond the mountains. As optimal datum we have considered the hourly rain measured during the event from about 130 raingauges located from 135° to 270° azimuth, i.e. in the Appennino zone, and 20 Km far from radar, to avoid the area of secondary lobes. The radar rain has been interpolated in a grid of 1 Km×1 Km of resolution and cumulated in the hour; the hourly datum of each raingauge has been compared with them of the radar in the correspondent cell. To convert Z in rain (R), we have used an equation of type Marshall and Palmer (1948), $Z{=}aR^b$. In absence of the optimum pair of coefficients a and b we have evaluated the performance of the two algorithms varying a and b.

Once defined the bias as

$$\langle \varepsilon_R \rangle = \langle R_R - R_P \rangle \tag{4}$$

the other calculated evaluation indexes are (Marzano et al., 2004) :

– the root mean square error

$$RMSE = \sqrt{\langle \varepsilon_R^2 \rangle} \tag{5}$$

– the fractional mean reduction

$$FMR = \frac{\langle R_P \rangle - \langle \varepsilon_R \rangle}{\langle R_P \rangle} \tag{6}$$

– the fractional variance reduction

$$FVR = \frac{\left\langle \sigma_{R_P}^2 \right\rangle - \left\langle \sigma_{\varepsilon_E}^2 \right\rangle}{\left\langle \sigma_{R_P}^2 \right\rangle} \tag{7}$$

– the mean ratio bias

$$MRB = \frac{\langle R_P \rangle}{\langle R_R \rangle} \tag{8}$$

The optimal value of FMR, FVR and MRB is 1 and of RMSE is 0. We have calculated this indexes using radar rain from the new algorithm (BSA) and from 'CAM + anaprop correction' algorithm (SA) and we have compared them. Fig. 10, Fig. 11 and Fig. 12 shows respectively the RMSE, the FMR

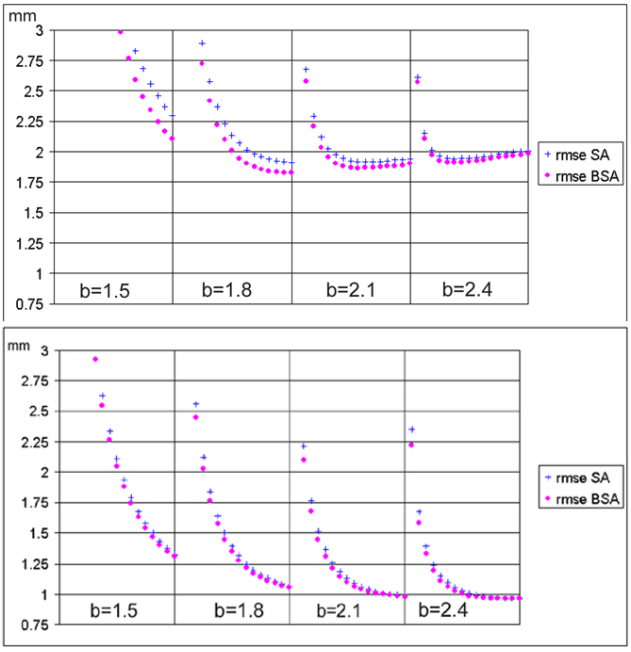

Fig. 10. RMSE of summer event (upper) and for winter event (below) for the CAM+anaprop algorithm (SA=static map+anaprop) and for the new algorithm (BSA=blocking +new static map +anaprop). In each *b*-constant sector, *a* increases from left to right, at step of 100, from 100 to 1600.

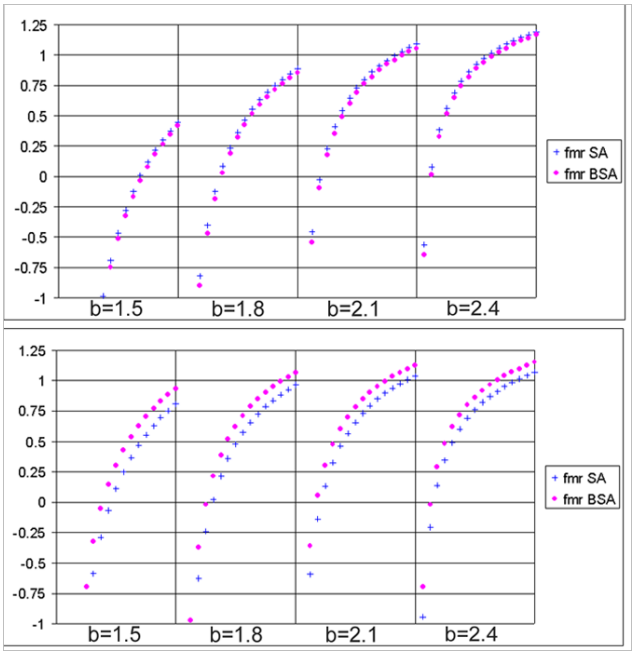

Fig. 11. FMR of summer event (upper) and for winter event (below) for the CAM+anaprop (SA) and for the new algorithm (BSA).

and FVR coupled with MRB, vs. MP coefficients *a* and *b*, for the two methods, in the two case study.

The new algorithm shows a lower RMSE moreover in the anaprop case of summer 2003. The amount of the improvement is closely dependent on the pair of chosen MP coefficient.

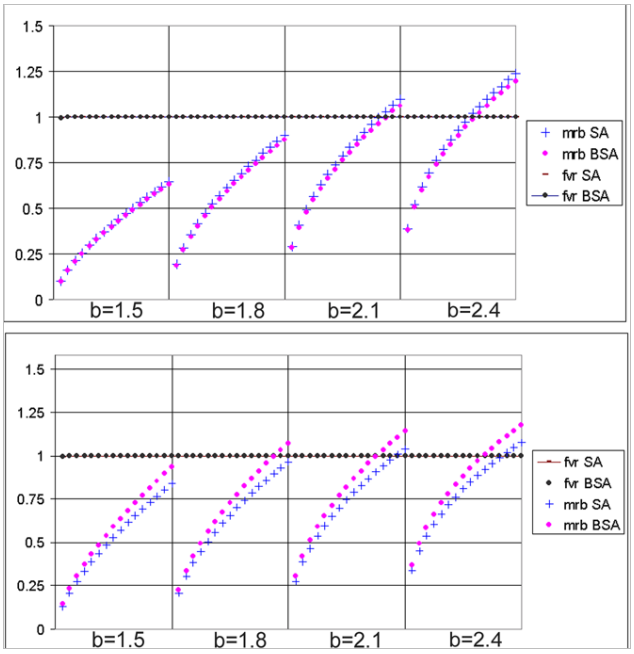

Fig. 12. FVR and MRB of summer event (upper) and for winter event (below) for the CAM+anaprop (SA) and for the new algorithm (BSA).

It is difficult to evaluate the performance of the algorithms observing the bias and similar indexes as FMR and MRB. This indexes are conditioned totally from *a* and *b*. FVR, in the analysed cases, is very near to 1 because the variance of the error is more smaller than the variance of the rain field. A strong influence on the value of this indexes has even the variation of vertical profile of reflectivity, that here is not corrected. In fact, the introduction of propagation and BB model, increases often the height at which the reflectivity data are kept, respect to the old algorithm. In an operational line, where the VPR is not corrected, this can imply for the final rain rate a smoothing of the previous improvement or even a worsening. Finally, it must be noted that the indexes are calculated on cells that are concentrated in the Appennino area into the region Emilia Romagna (Fig. 13); i.e. the performance of the algorithm in the boundary of the radar map is so neglected.

5 Conclusions

The illustrated correction schema introduces some advantages respect to the correction of the CAM+anaprop algorithm. At first, it takes into account the real (or approximated) atmospheric state and recognizes anomalous propagation conditions. This permit to change the elevation at wich the data are kept, avoiding or reducing this artifice, before the application of the anaprop removal algorithm. Second, it introduces the beam blockage correction and produces

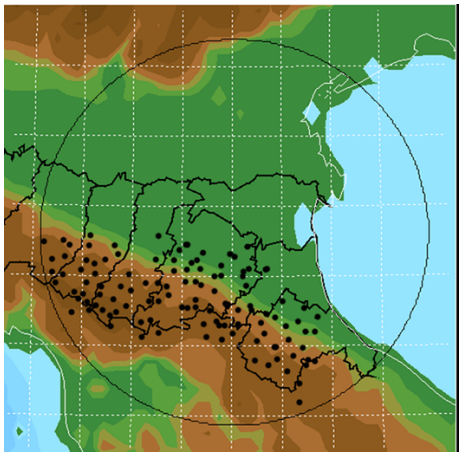

Fig. 13. Spatial distribution of the raingauges used for the statistical analysis.

a more reliable field after the mountains, reducing the shadowing effect of mountains and valleys. Further, the algorithm is simplex to implement and has a low computational cost. At end, it produces indicators of data quality that can be useful to evaluate its reliability in hydrological and meteorological applications such as data assimilation. Therefore the schema is suitable to an operational use but it must be integrated, before, with the correction of the vertical profile of reflectivity. Finally, to obtain the best field, very important is the choice of the Z-R relation, depending on the type of event, or at lest on the season.

Acknowledgement. The authors greatly acknowledge Mr. Joan Bech (MeteoCAT) for the ray propagation and beam blocking code. This work is partially supported by CARPE DIEM, a research project supported by the European Commission under the 5th FP (Contract No. EVG1-CT-2001-0045), and form the GNDCI through the project RAM.

References

Alberoni, P. P., Anderson, T., Mezzasalma, P., Michelson, D. B., and Nanni, S.: Use of the vertical reflectivity profile for identification of anomalous propagation, Meteorological Applications, 8, 257–266, , 2001.

Bean, B. R. and Dutton, E. J.: Radio Meteorology, Dover Publications, 435 pp., 1968.

Bech, J., Codina, B., Lorente, J., and Bebbington, D.: The sensitivity of single polarization weather radar beam blockage correction to variability in the vertical refractivity gradient, Journal of Atmospheric and Oceanic Technology, 20, 6, 845–855, 2003.

Doviak, R. J. and Zrnic, D. S.: Doppler radar and weather observations, Academic Press, 562 pp., 1993.

Marzano, F. S., Picciotti, E., and Vulpiani G.: Rain Field and Reflectivity Vertical Profile Reconstruction From C-Band Radar Volumetric, Data, Ieee transactions on geoscience and remote sensing, 42, 5, May 2004.

Marshall, J. S and Palmer, W. McK.: The distribution of raindrops with size, J. Meteor., 5, 165–166, WMO Publications, No. 9, Vol. C1 Catalogue of Meteorological Bulletins, 1948.